Stable Propagation of Solitons in Strongly Dispersion-Managed Unequal-Length Optical Fiber Link with Loss

Wenrui Xue, Guosheng Zhou, Zhonghao Li, and Shuqin Guo

***Abstract*—Using average approximation, we obtained a phase plane evolution picture of soliton propagated in strongly dispersion-managed optical fiber link with loss. After analyzed this picture, we proposed a new picture to keep soliton propagate stably in this system. Stable propagation parameters are given and twenty points we are interested in are selected. Using these parameters, we can construct any type of optical fiber link. Considering the length of article, we give two types of link with peak power 2 and 8 mW. With an input pulse train consisting of 32 bits in return-to-zero (RZ) format, numerical simulation has been done. We find that soliton can stably propagate through these optical fiber link constructed by ten unequal-length unit with a data rate of 13.33 Gb/s.**

***Index Terms*—Dispersion management, optical fiber link, phase plane evolution picture, soliton, unequal length.**

I. Introduction

RECENTLY ,many papers focus on dispersion-managed optical fiber link [1]–[10] because of its simplicity, compatibility with all optical transparency, convenience in link connection, superiority in reduction of Godon–Haus timing jitter, potentiality in application of wavelength-division-multiplexed (WDM) system with wavelength near zero dispersion, and easiness in upgrading of installed fiber lines to soliton-based fiber lines to increase middle and long distance communication capacity.

Generally speaking, real dispersion managed optical fiber links are made up of many unequal-length units. In each unit, several loss fiber segments and one amplifier are contained. However, almost all of theoretical works were involved with lossless fiber links that were made up of equal-length units. In this paper, we study unequal-length strongly dispersion-managed optical fiber link with loss, give stable propagation parameters of soliton in such system, and verify them with numerical simulation.

Manuscript received October 18, 1999; revised March 14, 2000. This work was supported in part by the National Natural Science Foundation of China, under Grant 69678011), the National Laboratory. on Local Fiber-Optic Communication Networks and Advanced Optical Communication System Foundation, and the Shanxi Provincial Science Foundation.

The authors are with Department of Electronics and Information Science, Shanxi University, Taiyuan, Shanxi 030006, China (e-mail: wrxue@mail.sxu.edu.cn).

Publisher Item Identifier S 0733-8724(00)05767-4.

II. Basic Theory

The evolution of a pulse propagated in an optical fiber with loss and weak Kerr nonlinearly is described by the nonlinear Schrödinger equation,

$$i\frac{\partial u}{\partial z} - \frac{1}{2}\beta_i\frac{\partial^2 u}{\partial t^2} + \gamma|u|^2u + \frac{i}{2}\alpha u = 0 \tag{1}$$

where β_i is the group velocity dispersion, γ is the Kerr nonlinear coefficient, α is the loss coefficient, z is the distance of propagation, t is the time in the group-velocity frame, and the subscripts i denote the parameters related to different fiber segments in one unit. Here, we assume that the attenuation is same in all segments.

Let $u = \exp(-\alpha z/2)\psi$, we can obtain

$$i\frac{\partial \psi}{\partial z} - \frac{1}{2}\beta_i\frac{\partial^2 \psi}{\partial t^2} + \gamma'|\psi|^2\psi = 0. \tag{2}$$

Here, $\gamma' = \gamma\exp(-\alpha z)$. The pulse is assumed to be hyperbolic secant

$$u(z,t) = A(z)\operatorname{sech}\left[\frac{t}{T(z)}\right]\exp\left[-i\frac{c(z)t^2}{2T^2(z)}\right] \tag{3}$$

where $A(z), T(z)$ and $c(z)$ indicate the pulse's amplitude, duration and chirp, respectively.

A. Lossless Case

In lossless case $(\alpha = 0.0)$, assuming the configuration of one unit is DCF + SMF + SMF + DCF, the phase evolution equation for each segment can be obtained using variational method, also see [3], [4],

$$-\frac{c_i^2}{4/\pi + N^2/H_i} + \frac{(T_i - \beta_i N/H_i)^2}{\beta_i^2(4/\pi + N^2/H_i)/H_i} = 1 \tag{4}$$

where $H_i = \beta_i^2(4/\pi^2 + c_i^2)/T_i^2 + 2\beta_i N/T_i$, and it is constant in each segment during propagation. $N = 4\gamma P_0 T_0/\pi^2 \cdot P_0$ and T_0 are initial peak power and duration respectively. c_i and T_i is chirp and duration respectively. The subscripts i denote the parameters related to the different segments $(i = 1, 2, 3, 4)$.

The phase plane evolution picture of the pulse propagating in different segments in one unit is shown in Fig. 1, also see [3]. Based on this picture, we can design unequal-length optical fiber

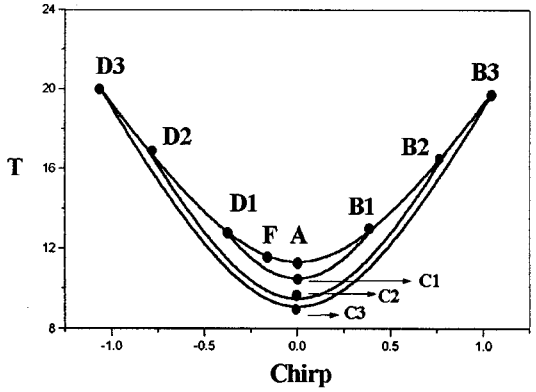

Fig. 1. Phase plane evolution picture of the pulse propagated in a lossless optical fiber link with three fiber segments within one unit.

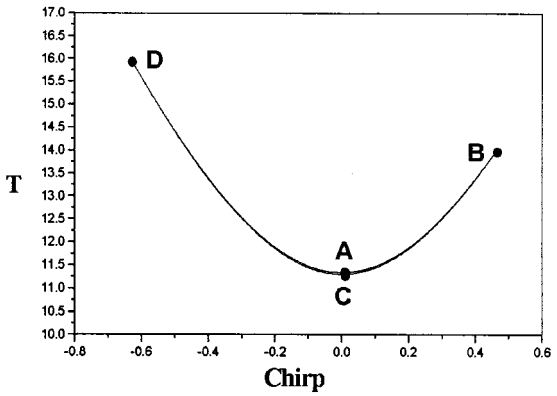

Fig. 2. Phase plane evolution picture of the pulse propagated in a loss optical fiber link with three fiber segments within one unit.

links. The hyperbola D_iA and AB_i are corresponding to the dispersion compensating fiber (DCF), B_iC_i and C_iD_i are corresponding to the standard monomode fiber (SMF). The point F is a starting point, and optical pulse propagates by FAB_i in DCF and by $B_iC_iD_i$ in SMF, thus in the next piece of DCF it will return to point F with the same values of $T_i(F)$ and $c_i(F)$ as the initial ones $(i = 1, 2, 3)$. Obviously, the basic requirement of the optical fiber link with dispersion compensation lies in that the pulse duration and chirp should have nearly the same values at the beginning and the end points of each unit. The starting point F must be at the shortest unit D_1AB_1, otherwise the same values of the pulse durations can not be obtained at the ends of different units.

Since the best starting point is the point A with zero chirp, we will discuss this case. For example, let us analysis the phase picture $AB_1C_1D_1A$ in Fig. 1. By using the symmetry property for the time durations and antisymmetric property for the chirps at points B_1 and $D_1, T(B_1) = T(D_1)$ and $c(B_1) = -c(D_1)$, (5) can be given analytically using variational method, also see [5]

$$H_iL_i = \sqrt{H_i} f[T(B_1), H_i] + \beta_i N \cdot \ln\left\{ \frac{[f[T(B_1), H_i] + T(B_1) - \beta_i N/H_i}{T(A) - \beta_i N/H_i} \right\} \Big/ \sqrt{H_i} \tag{5}$$

where $f[T(B_1), H_i] = [T^2(B_1) - 2\beta_i N T(B_1)/H_i - 4\beta_i^2/(\pi^2 H_i)]^{1/2}$ and

$$H_i = \beta_i^2 \left(4/\pi^2 + c_i^2(B_1)\right)/T_i^2(B_1) + 2\beta_i N/T_i(B_1). \tag{6}$$

Here i denote the segment AB_1 and CD_1, L_i denote the lengths of AB_1 or C_1D_1.

From (5) and (6), dependence of average dispersion $\beta_{\mathrm{AV}} = \sum \beta_i L_i / \sum L_i$, $(i = 1, 2, 3, 4)$, length of DCF(L_{DCF}) and length of SMF(L_{SMF}) on soliton's peak power (P_0) and soliton's width at point B ($T(B)$) can be calculated.

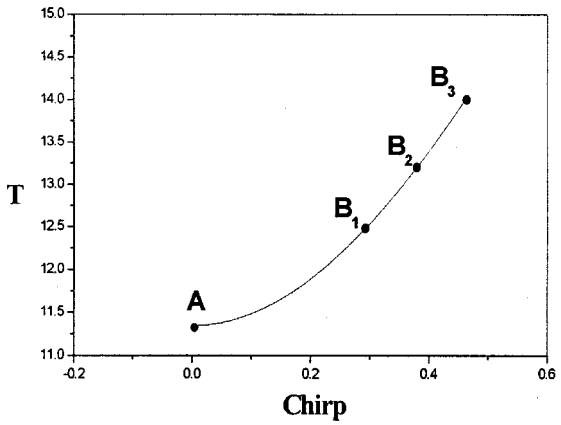

Fig. 3. Phase plane evolution picture of the pulse propagated in a loss optical fiber link with two fiber segments within one unit.

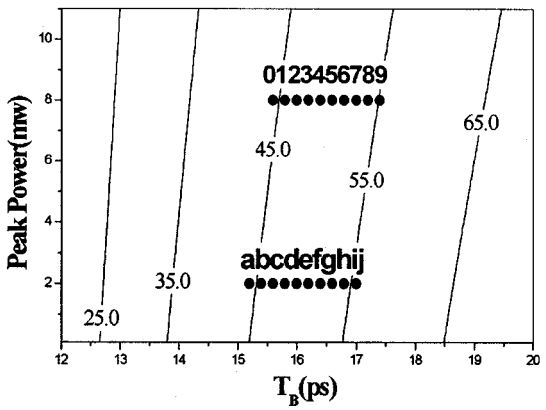

Fig. 4. Contour plot of L_{DCF} (km) as a function of $T(B)$ and P_0 when we use DCF-SMF as one unit.

B. Loss Case

In loss case $(\alpha \neq 0.0)$, Assume the configuration of one unit is DCF + SMF + SMF + DCF + EDFA, here EDFA is used to compensate for the loss in the unit. The total gain of the amplifier is $\exp(\alpha(L_{\mathrm{DCF}} + L_{\mathrm{SMF}} + L_{\mathrm{SMF}} + L_{\mathrm{DCF}}))$. Here, we can use average approximation method. Substituting γ with γ', one can finds that all the result from (4) to (6) can be used for

TABLE I
PARAMETERS OF SELECTED TEN POINTS WITH $P_0 = 2$ mW

Points	T(B)(ps)	P_0(mw)	L_{DCF}(Km)	L_{SMF}(Km)	$\beta_{AV}(ps^2/Km/nm)$
a	15.2	2	44.249	45.177	-0.0415
b	15.4	2	45.567	46.500	-0.0405
c	15.6	2	46.865	47.803	-0.0396
d	15.8	2	48.145	49.087	-0.0387
e	16.0	2	49.408	50.355	-0.0379
f	16.2	2	50.656	51.606	-0.0372
g	16.4	2	51.888	52.843	-0.0364
h	16.6	2	53.108	54.066	-0.0357
i	16.8	2	54.315	55.277	-0.0351
j	17.0	2	55.510	56.475	-0.0345

TABLE II
PARAMETERS OF SELECTED TEN POINTS WITH $P_0 = 8$ mW

Points	T(B)(ps)	P_0(mw)	L_{DCF}(Km)	L_{SMF}(Km)	$\beta_{AV}(ps^2/Km/nm)$
0	15.6	8	44.378	48.139	-0.1626
1	15.8	8	45.623	49.409	-0.1594
2	16.0	8	46.853	50.663	-0.1563
3	16.2	8	48.068	51.901	-0.1534
4	16.4	8	49.270	53.126	-0.1506
5	16.6	8	50.460	54.337	-0.1480
6	16.8	8	51.638	55.537	-0.1455
7	17.0	8	52.805	56.725	-0.1432
8	17.2	8	53.963	57.903	-0.1409
9	17.4	8	55.110	59.069	-0.1387

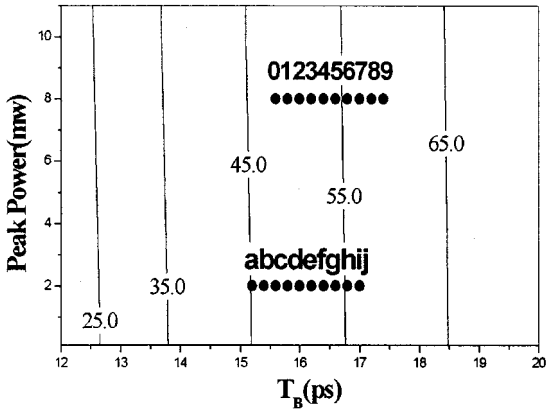

Fig. 5. Contour plot of $L_{\rm SMF}$ (km) as a function of $T(B)$ and P_0 when we use DCF-SMF as one unit.

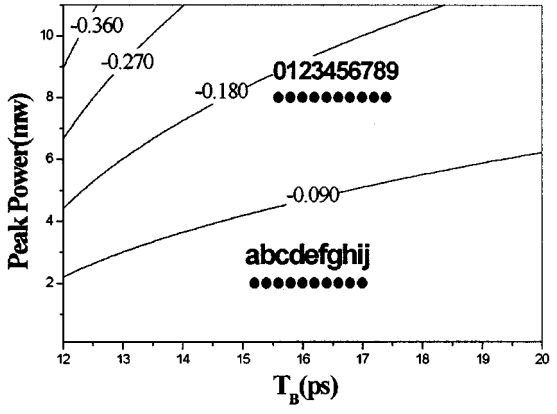

Fig. 6. Contour plot of $\beta_{\rm AV}$ ps^2/km/nm as a function of $T(B)$ and $P(0)$ when we use DCF-SMF as one unit.

loss case. Let

$$
\begin{aligned}
N_1' &= \frac{4P_0T_0\gamma}{\pi^2L_1'} \quad \int_0^{L_1'} \exp(-\alpha z)\,dz \\
N_2' &= \frac{4P_0T_0\gamma}{\pi^2L_2'} \quad \int_{L_1'}^{L_1'+L_2'} \exp(-\alpha z)\,dz \\
N_3' &= \frac{4P_0T_0\gamma}{\pi^2L_3'} \quad \int_{L_1'+L_2'}^{L_1'+L_2'+L_3'} \exp(-\alpha z)\,dz \\
N_4' &= \frac{4P_0T_0\gamma}{\pi^2L_4'} \quad \int_{L_1'+L_2'+L_3'}^{L_a} \exp(-\alpha z)\,dz \qquad (7)
\end{aligned}
$$

where L_i' denote the length of each segment, and $L_a = L_1' + L_2' + L_3' + L_4'$ is the total length of one unit. Hence, we can increase α from $\alpha = 0.0$ (lossless case) to $\alpha = 0.046$ (real value) by iterating (5) and (7).

Fig. 2 is a phase plane evolution picture with $T(A) = 11.344$ ps, $T(B) = 14.0$ ps, $P_0 = 2.0$ mW, $\beta_{\rm DCF} = 4$ ps^2/km, $\beta_{\rm SMF} = -4$ ps^2/km, $\gamma = 1.27$/km/W, and $\alpha = 0.046$. We can see that phase plane evolution picture become asymmetrical, $T(D) > T(B)$. We also find that $T(C)$ is close to $T(A)$ little by little, and $T(D)$ become more and more larger than $T(B)$ when α is increasing. This phenomenon can be explained with effective nonlinearly. Because $\gamma' = \gamma \exp(-\alpha z)$, effective nonlinearity is related with propagation distance z, and the value of

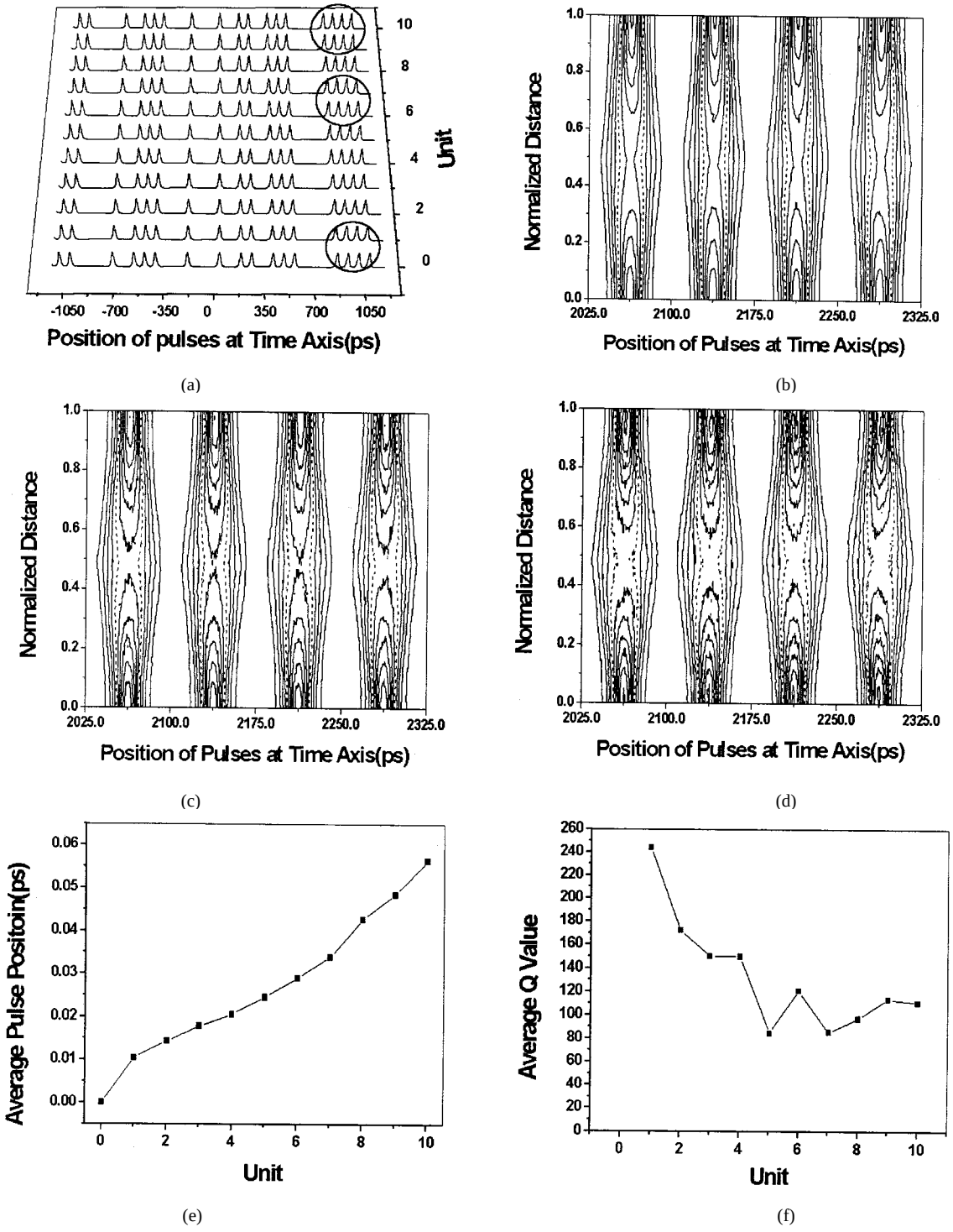

Fig. 7. (a) Waveforms of one random pulse train with 2 mW peak power at the end of each unit. We selected three units that marked by three circles to analysis the effect of soliton-soliton interaction. (b), (c), and (d) is the contour plot of waveform versus position of pulse at time axis and normalized distance of first, second, and last circle marked unit along unit respectively. (e) is average pulse position versus unit. (6) is averaged Q value versus unit.

γ' gradually descends when z increases. In order to keep the balance of dispersion and nonlinearity, L_3' and L_4' must be larger than that in the lossless case. In fact, giving $T(A), T(B)$, and P_0, increasing α from 0.0 to 0.046, $T(D)$ will be approaching an unacceptable value to satisfy the condition that the pulse duration and chirp should have nearly the same value at the beginning and the ending point of each unit.

In view of this, we can use a new phase plane evolution picture, see Fig. 3. There are two fiber segments within one unit, the first segment is DCF, and the followed is SMF. A is the start point, soliton propagates by AB in DCF, then it return to A by BA in SMF. According to this new phase plane evolution picture, we can give stable propagation parameters by using the same iterating method mentioned above.

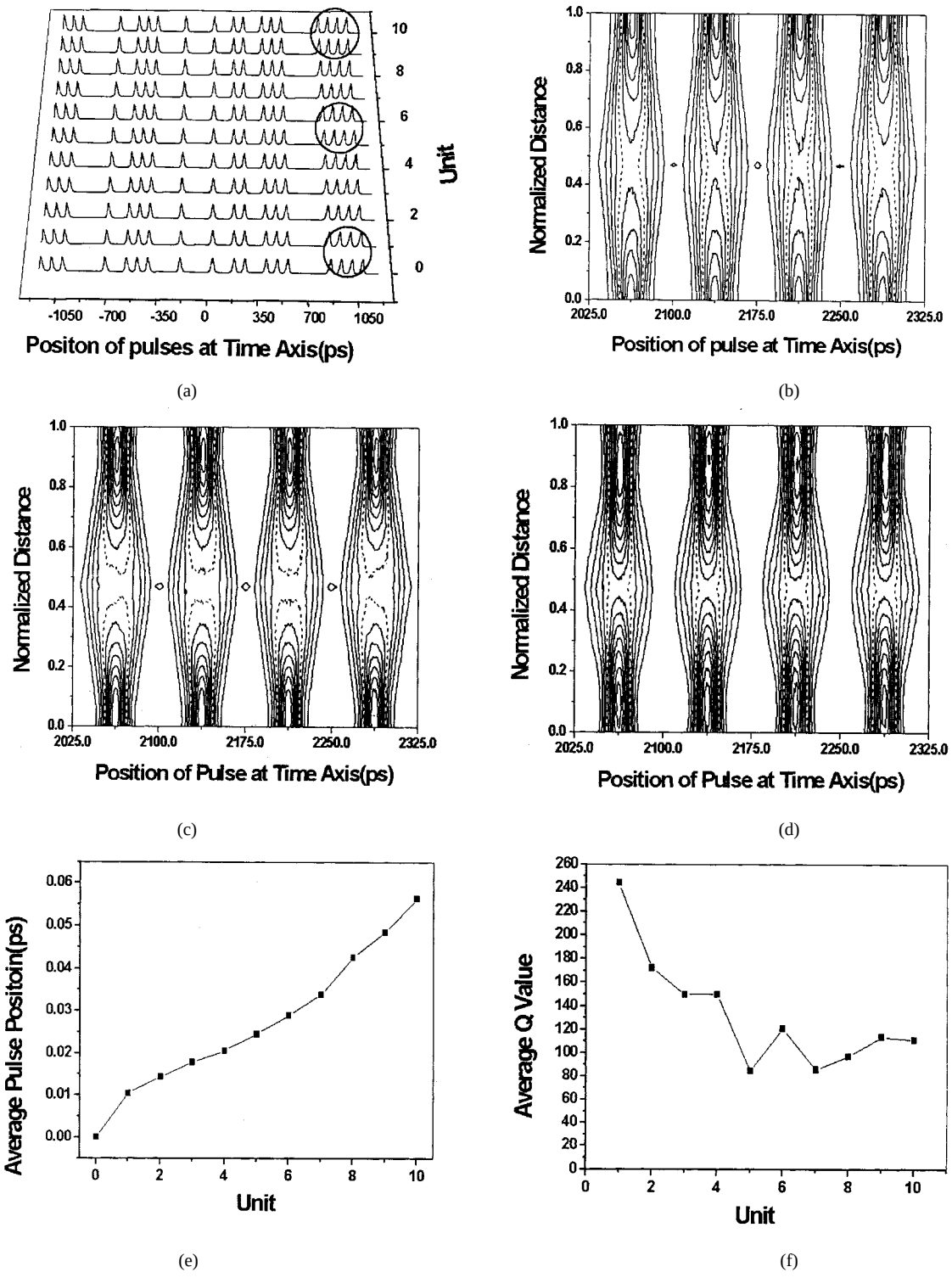

Fig. 8. (a) Waveforms of one random pulse train with 8-mW peak power at the end of each unit. We selected three units that marked by three circles to analysis the effect of soliton-soliton interaction. (b), (c), and (d) is the contour plot of waveform versus position of pulse at time axis and normalized distance of first, second, and last circle marked unit along unit, respectively. (e) is average pulse position versus unit. (f) is averaged Q value versus unit.

We want to seek stable propagation condition under one premise: amplifiers are spaced about 100 km within one 1000-km-long optical fiber link, there is one amplifier and two segment fibers within one unit. Because long amplifier spacing is beneficial from the economical point of view. Figs. 4, 5 and 6 are contour plot of length of DCF($L_{\rm DCF}$), length of SMF($L_{\rm SMF}$) and average dispersion $\beta_{\rm AV}$ vs soliton's peak power (P_0) and soliton's width at point $B(T(B))$, respectively.

From Figs. 4–6, we can see that the region we are interested in is $15\ {\rm ps} < T(B) < 18\ {\rm ps}$, $0.1{\rm mW} < P_0 < 11.0\ {\rm mW}$ when we chose the following parameters: $T_0 = 11.344$ ps ($T_{\rm FWHM} = 20$ ps), $\beta_{\rm DCF} = 4\ {\rm ps}^2/{\rm km}$, $\beta_{\rm SMF} = -4\ {\rm ps}^2/{\rm km}$, $\gamma = 1.27/{\rm km/W}$,

$\alpha = 0.046$, and $c(0) = 0.0$. In this region, we can select parameters to design real strongly dispersion-managed unequal-length optical fiber link with loss.

III. Numerals Results

In order to verify above results, we solved (2) by split-step numerical method to simulate real unequal strongly dispersion-managed optical fiber link. We chose 20 points (a, b, c, d, e, f, g, h, i, j and 0, 1, 2, 3, 4, 5, 6, 7, 8, 9) from Fig. 4. Their corresponding positions are also shown in Figs. 5 and 6. and their corresponding parameters are shown in Tables I and II. From these two tables, we can see that the length of one unit is about 85–115 km.

Using these parameters, any types of unequal-length optical fiber link can be constructed. Considerring the length of article, we give two examples here. We can construct arbitrarily two type 1000-km-long links: c+f+i+j+b+e+a+g+d+h with 2-mW peak power, and 7+2+5+0+4+9+1+8+3+6 with 8-mW peak power.

We injected a chirp-free pulse train with 32 return-to-zero (RZ) pseudorandom solitons into the optical fiber link. The pulse train is 2400-ps long, with each bit occupying a 75-ps time slot corresponding to a data rate of 13.33 Gb/s. The effects of amplified-spontaneous-emission (ASE) noise of the EDFA is modeled by addition of noise in the Fourier domain immediately after the amplifiers. We add an amount of noise $\delta u = A\exp(i\varphi)$ to each Fourier component, where $A = (n_{\rm sp}h\nu(G-1)\Delta\nu)^{1/2}$, $n_{\rm sp}$ is spontaneous-emission coefficient, h is Plank constant, ν is frequency, G is the total gain of the amplifier, φ is a random phase from 0 to 2π, and $\Delta\nu$ is the bandwidth associated with each Fourier component [11]. We did not include any filter in our simulation.

The performance of our simulated system are evaluated by calculating the waveform, the position of pulse at time axis and the Q factor. The Q factor is defined as

$$Q = \frac{\mu_1 - \mu_0}{\sigma_1 + \sigma_0}$$

where the mean values μ_1 and μ_0 and the standard deviation σ_1 and σ_0 of the mark and space level are evaluated at the output of the optical pulse train. Fig.7(a) are waveforms of one random pulse train with 2-mW peak power at the end of each unit. We selected three units that marked by three circles to analysis carefully the effect of soliton-soliton interaction. Fig. 7(b), (c), and (d) is the contour plot of waveform versus position of pulse at time axis and normalized distance of first, second and last circle marked unit along unit respectively. On theses figure, the dot lines indicate the normalized height of 0.5. Fig. 7(e) is average pulse position versus unit. Fig. 7(f) is averaged Q value versus unit. Fig. 7(e) and (f) are results of average of 160 optical pulses' Monte Carlo simulations.

Fig. 8(a) are waveforms of one random pulse train with 8-mW peak power at the end of each unit. We selected three units that marked by three circles to analysis carefully the effect of soliton–soliton interaction. Fig. 8(b), (c), and (d) is the contour plot of waveform versus position of pulse at time axis and normalized distance of first, second and last circle marked unit along unit respectively. On theses figure, the dot lines indicate the normalized height of 0.5. Fig. 8(e) is average pulse position versus unit. Fig. 8(f) is averaged Q value versus unit. Fig. 8(e) and (f) are results of average of 160 optical pulses' Monte Carlo simulations.

From Figs. 7(a) and 8(a), we can see that solitons can keep their shape well at the end of each unit. From Fig. 7(b)–(d), Fig. 8(b)–(d), we can see that pulses' width are broadened and their peaks are descended due to soliton-soliton interaction. The higher the peak power of the input pulse is, the stronger the effect of soliton–soliton interaction is. But these changes do not effect waveforms at the end of each unit. So the deterioration due to interaction is not noticeable under the condition that we use 13.33 Gb/s data rate. From Fig. 7(e), (f) and Fig. 8(e), (f), we can see that performance of this kind of system is well. Q is very bigger and timing jitter is very smaller. The numerical simulation result in Figs. 7 and 8 showed that soliton can stably propagate through these 1000 km unequal-length optical fiber link with a data rate of 13.33 Gb/s.

IV. Conclusion

In conclusion, we used an average approximation method to deal with strongly dispersion-managed soliton propagation in optical fiber link with loss. We find that, in the loss case, the phase plane evolution picture is asymmetrical. Using the new phase plane evolution picture, stable propagation parameters are given and twenty points we are interested in are selected. Using these parameters of selected points, we constructed arbitrarily two types of optical fiber link with unit length from 85 to 115 km and peak power 2 or 8 mW. Numerical simulation proved that soliton can stably propagate through these 1000 km unequal-length optical fiber link with a data rate of 13.33 Gb/s.

References

[1] J. H. B. Nijhof, N. J. Doran, W. Forysiuk, and F. M. Knox, "Stable soliton-like propagation in dispersion managed systems with net anomalous, zero and normal dispersion," *Electron. Lett.*, p. 1726, 1997.

[2] F. Favre, D. L. Guen, and T. Georges, "20 Gbit/s soliton transmission over 5200Km of non-zero-dispersion-shifted fibre with 106 Km dispersion-compensated span," *Electron. Lett.*, vol. 34, p. 201, 1998.

[3] J. N. Kutz and S. G. Evangelides, "Dispersion-managed breathers with average normal dispersion," *Opt. Lett.*, vol. 23, p. 685, 1998.

[4] B. A. Malomed, "Pulse propagation in a nonlinear optical fiber with periodically modulated dispersion: variational approach," *Opt. Commun.*, vol. 136, p. 313, 1997.

[5] V. S. Grigoryan and C. R. Menyuk, "Dispersion-managed solitons at normal average dispersion," *Opt. Lett.*, vol. 23, p. 609, 1998.

[6] A. Berntson, N. J. Doran, W. Forysiak, and J. H. B. Nijhof, "Power dependence of dispersion-managed solitons for anomalous, zero and normal path-average dispersion," *Opt. Lett.*, vol. 23, p. 900, 1998.

[7] Y. Chen and H. A. Haus, "Dispersion-managed solitons with net positive dispersion," *Opt. Lett.*, vol. 23, p. 1013, 1998.

[8] S. K. Turitsyn and E. G. Shapiro, "Dispersion-managed solitons in optical amplifier transmission systems with zero average dispersion," *Opt. Lett.*, vol. 23, p. 682, 1998.

[9] T. Yu, R. M. Mu, V. S. Grigoryan, and C. R. Menyuk, "Energy enhancement of dispersion-managed solitons in optical fiber transmission systems with lumped amplifiers," *IEEE Photon. Technol. Lett.*, vol. 11, p. 75, 1999.

[10] H. Sugahara, T. Inoue, A. Maruta, and Y. Kodama, "Optical dispersion management for wavelength-division-multiplexed RZ optical pulse transmission," *Electron. Lett.*, vol. 34, p. 902, 1998.

[11] R. M. Mu, V. S. Grigoryan, C. R. Menyuk, E. A. Golovchenko, and A. N. Plipetski, "Timing-jitter reduction in a dispersion-managed soliton system," *Opt. Lett.*, vol. 23, p. 930, 1998.

Wenrui Xue was born in Hequ, Shanxi, China, in 1967. He received the B.S. degree in physics from the Shanxi Normal University, Linfen, Shanxi, China, in 1990, and the M.S. degree in physics from the Shandong University, Ji'nan, Shandong, China, in 1993, where he is now pursuing the Ph.D. degree in electronics engineering from the Shanxi University, Taiyuan, Shanxi, P.R.China.

His present research interests are in high-speed optical signal processing and fiber-optics communication systems.

Guosheng Zhou as born in Shanghai, China, in 1935. He received the B.S. degree in electronics from Peking University, Beijing, China, in 1959.

He is currently a Professor in the Department of Electronics and Information Science of Shanxi University, Taiyuan, Shanxi, China. His present research interests are in ultrafast phenomena, nonlinear optics, high-speed optical signal processing and fiber optics communication systems.

Zhonghao Li, photograph and biography not available at the time of publication.

Shuqin Guo, photograph and biography not available at the time of publication.